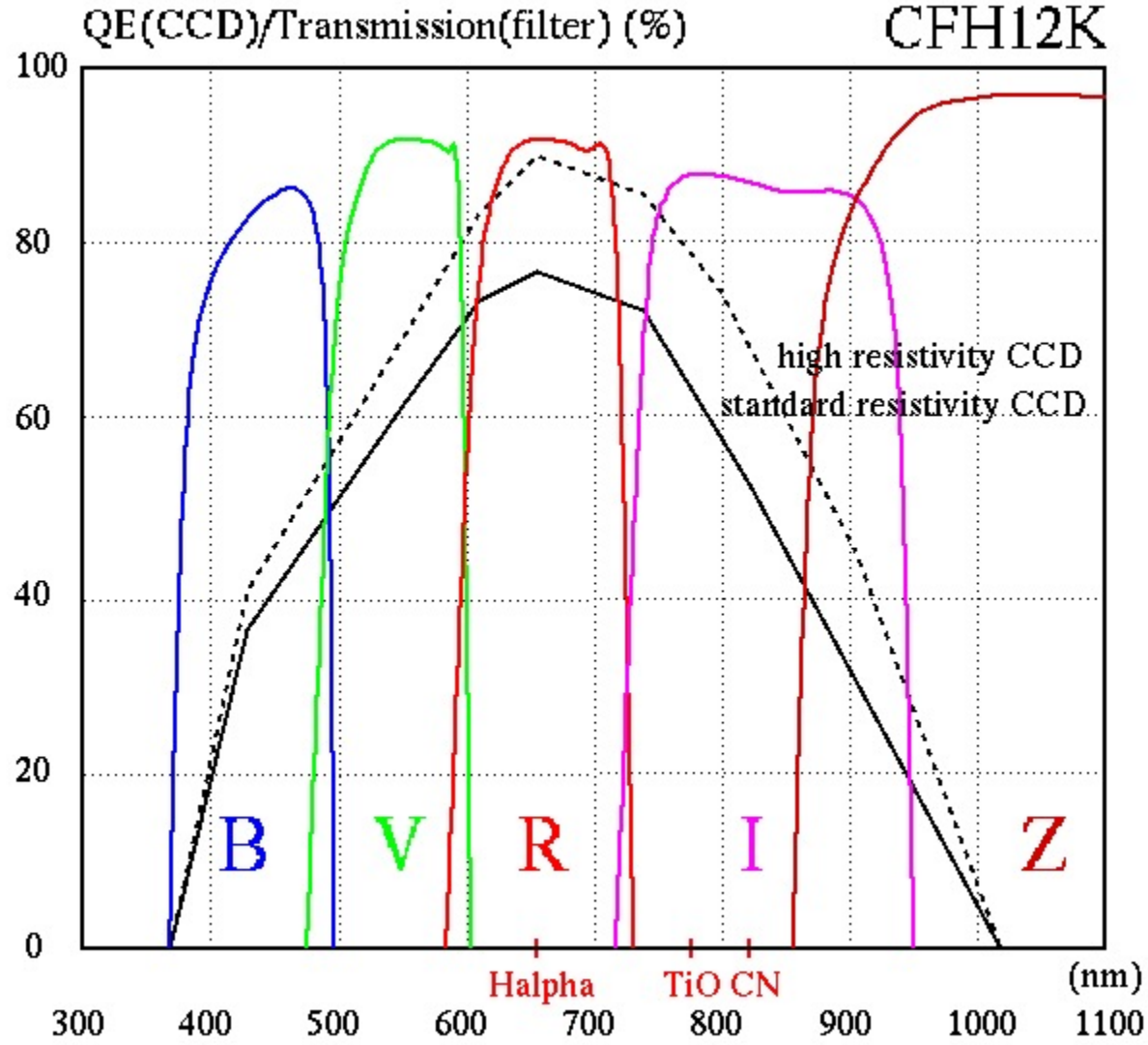


Strumentazione Astronomica: CCD



Strumentazione Astronomica: CCD

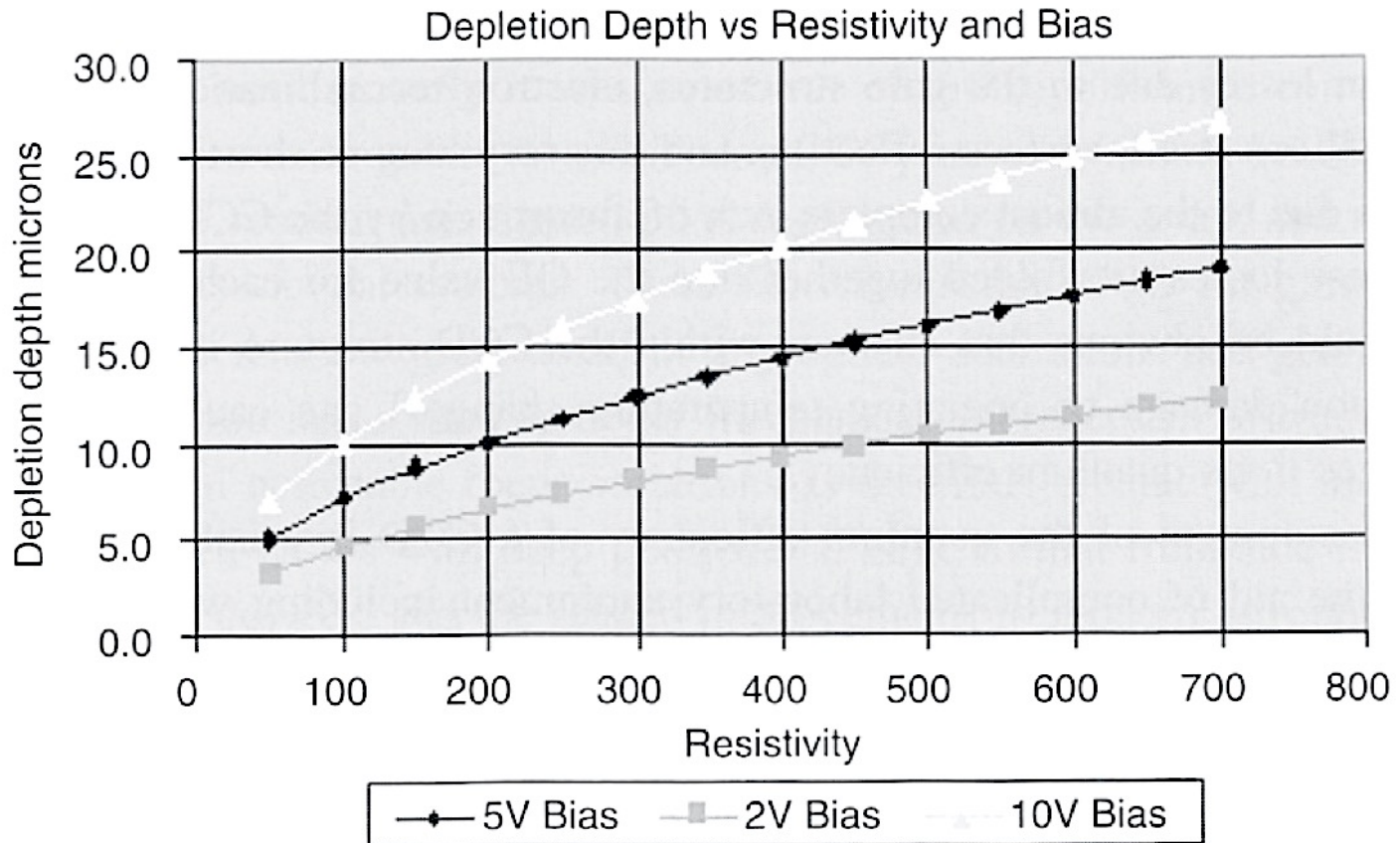
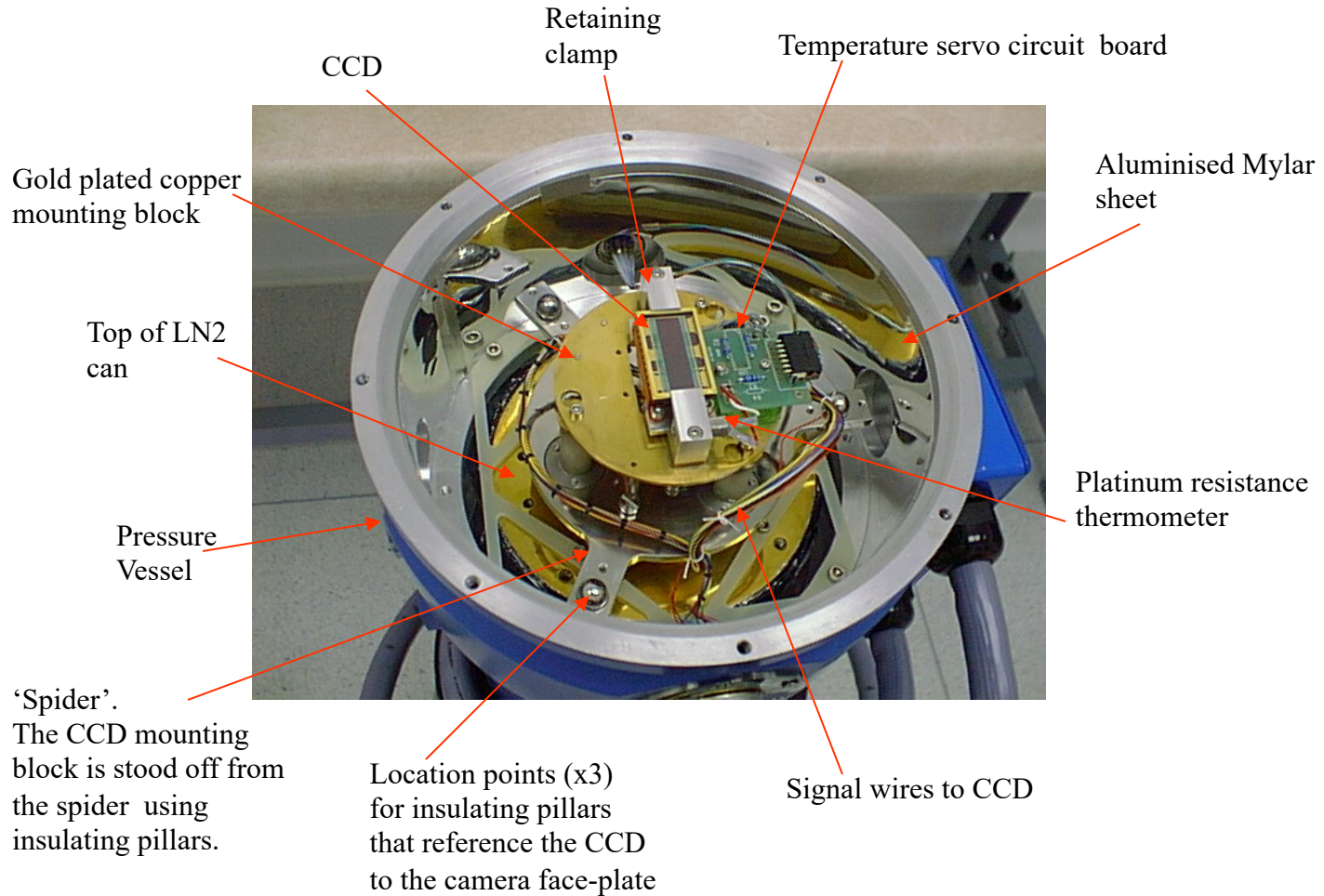


Fig. 3.5. Laboratory measurements of the depletion depth in a pixel vs. the CCD silicon resistivity for three different bias voltages. We see that one can deplete deeper (larger) pixels with higher resistivity silicon assuming the use of a larger bias voltage.

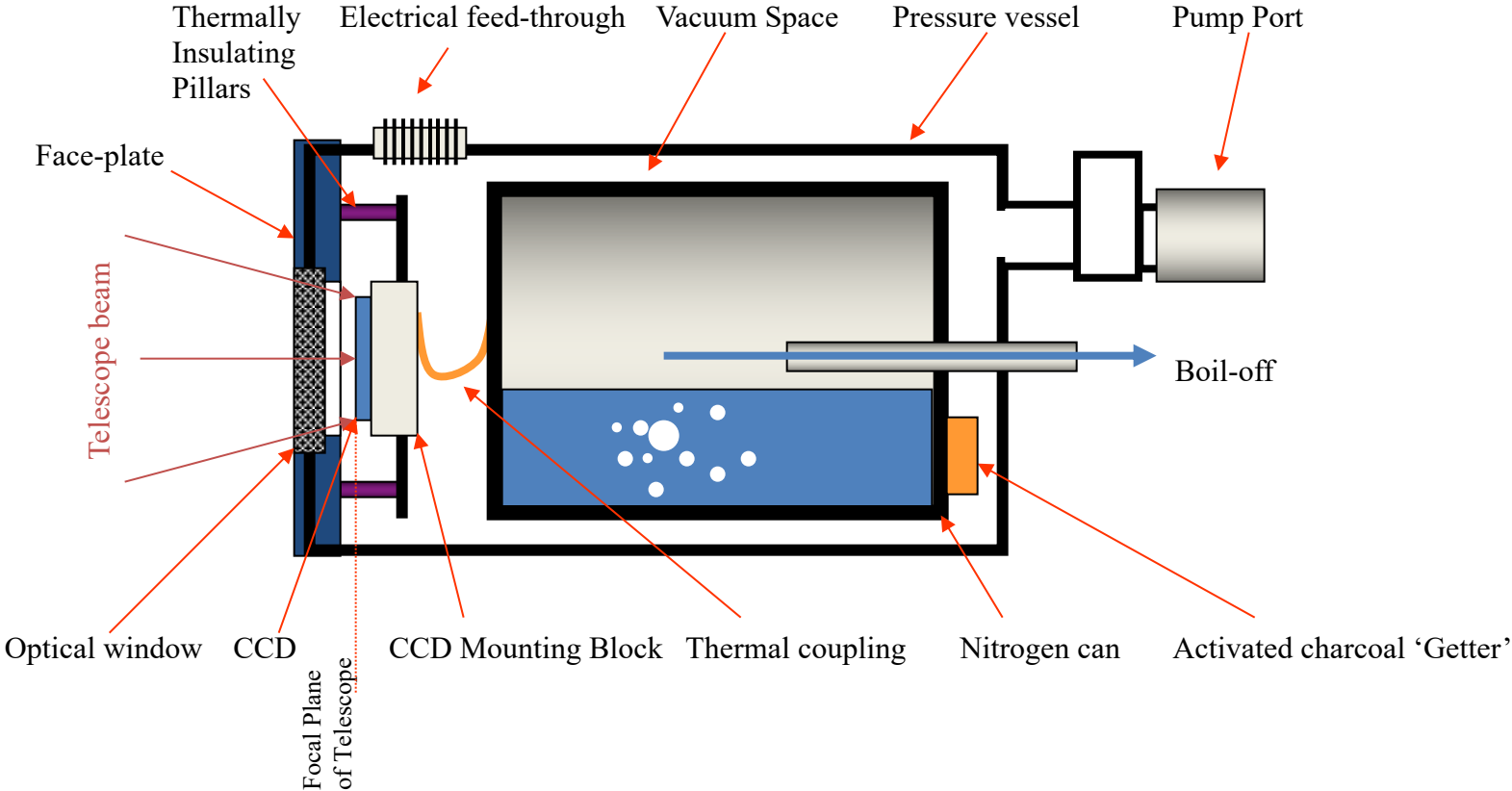
Strumentazione Astronomica: CCD

I CCD scientifici vengono raffreddati

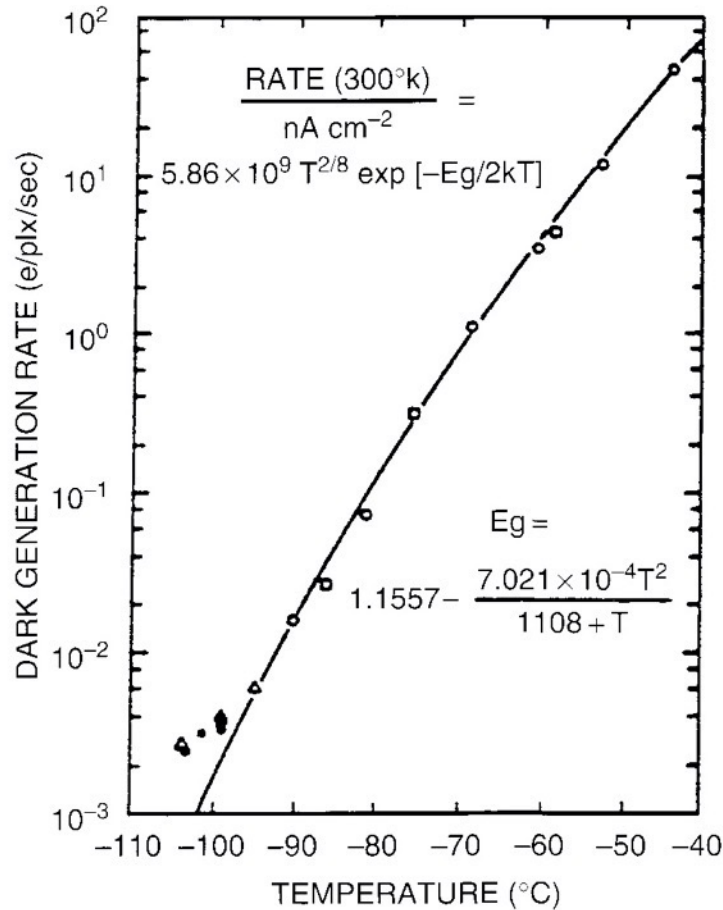


Strumentazione Astronomica: CCD

I CCD scientifici vengono raffreddati



Strumentazione Astronomica: CCD

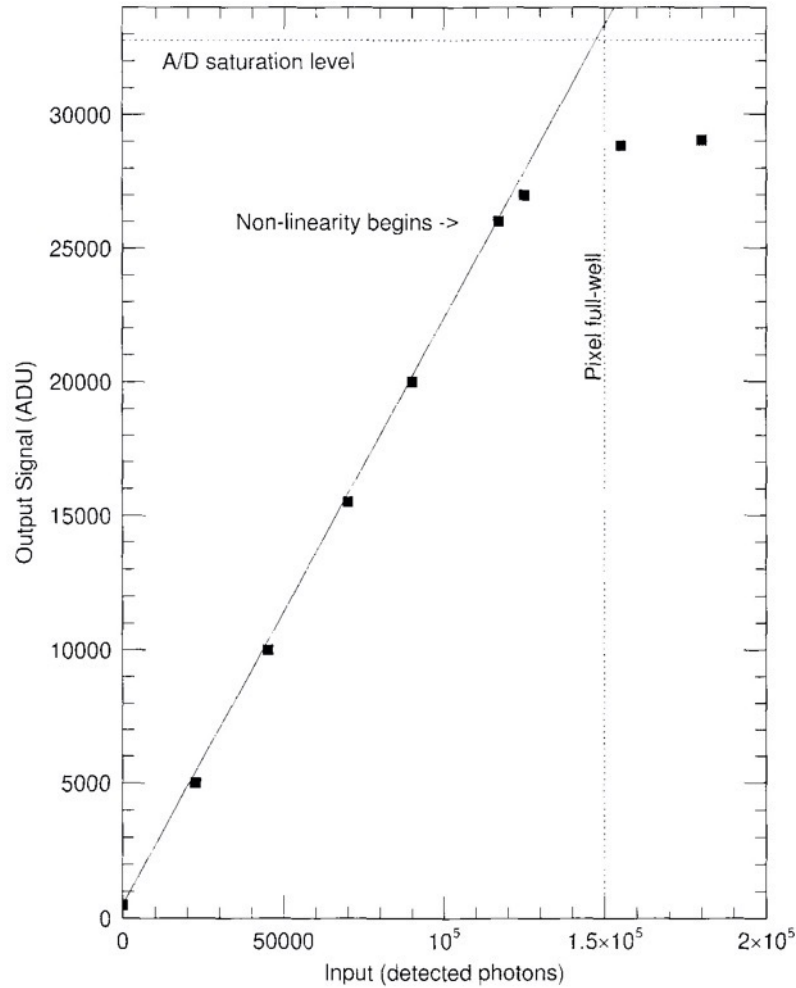


Fortemente dipendente da T

$DN_{\text{dark}} \approx e^{\alpha T}$ (thousands of e-/sec typical at room T)
 DN_{dark} typically doubles for every $\Delta T \approx 5\text{-}10^\circ\text{C}$

Fig. 3.6. Experimental (symbols) and theoretical (line) results for the dark current generated in a typical three-phase CCD. The rate of dark current, in electrons generated within each pixel every second, is shown as a function of the CCD operating temperature. E_g is the band gap energy for silicon. From Robinson (1988a).

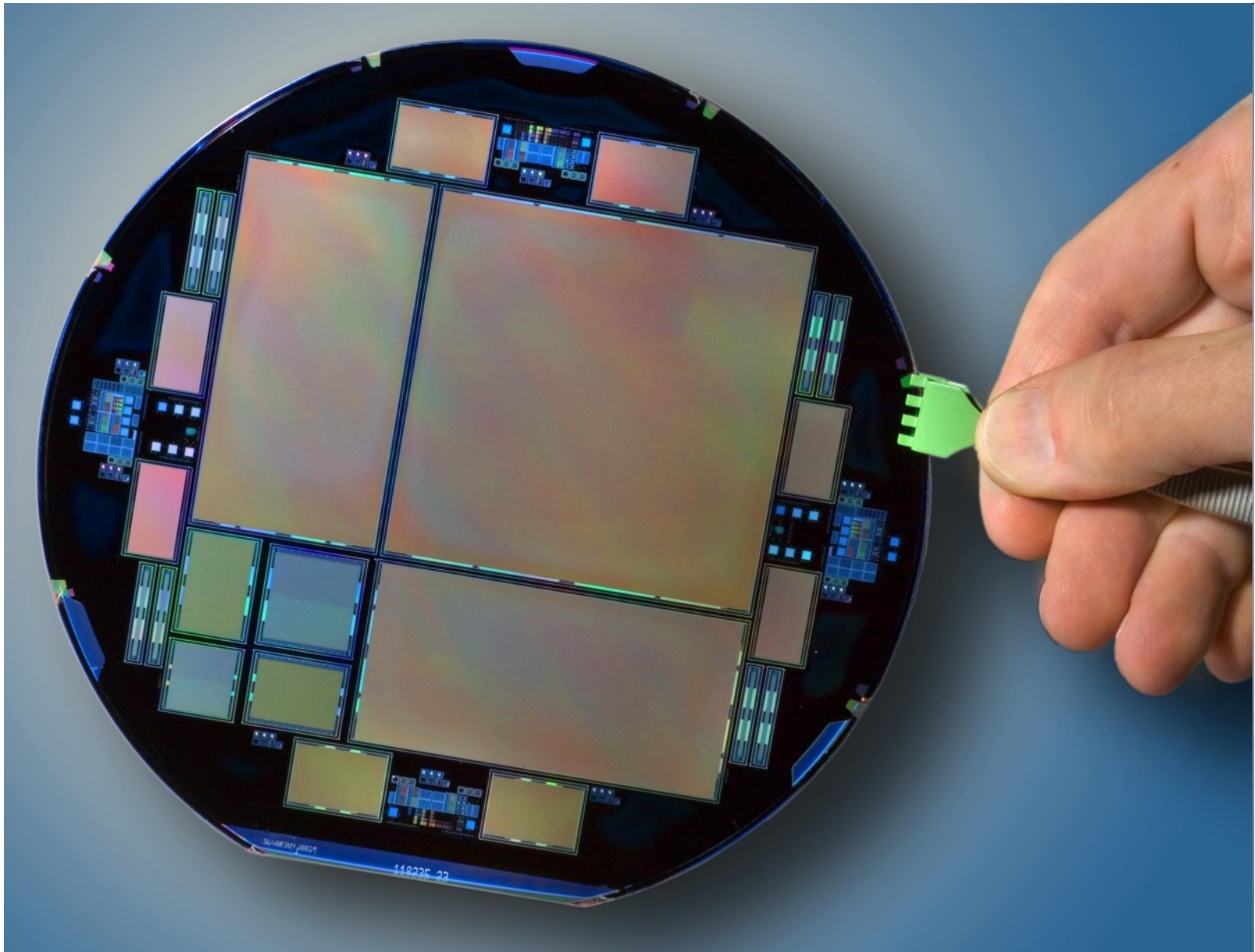
Strumentazione Astronomica: CCD



Linearità: un requisito
fondamentale per la fotometria

Fig. 3.9. CCD linearity curve for a typical three-phase CCD. We see that the device is linear over the output range from 500 ADU (the offset bias level of the CCD) to 26 000 ADU. The pixel full well capacity is 150 000 electrons and the A/D converter saturation is at 32 767 ADU. In this example, the CCD nonlinearity is the limiting factor of the largest usable output ADU value. The slope of the linearity curve is equal to the gain of the device.

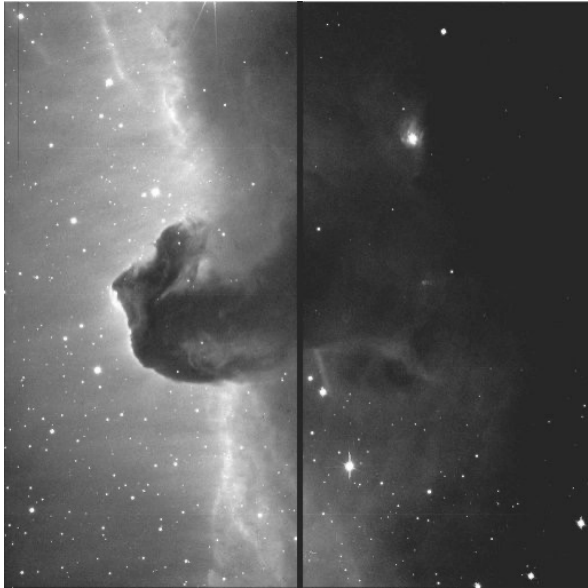
Strumentazione Astronomica: CCD



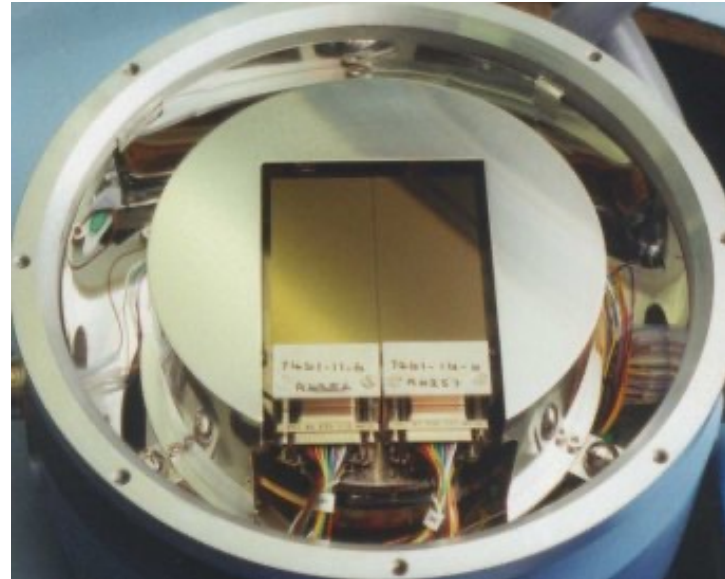
Strumentazione Astronomica: CCD

Mosaici di CCD

The Horsehead Nebula in Orion.

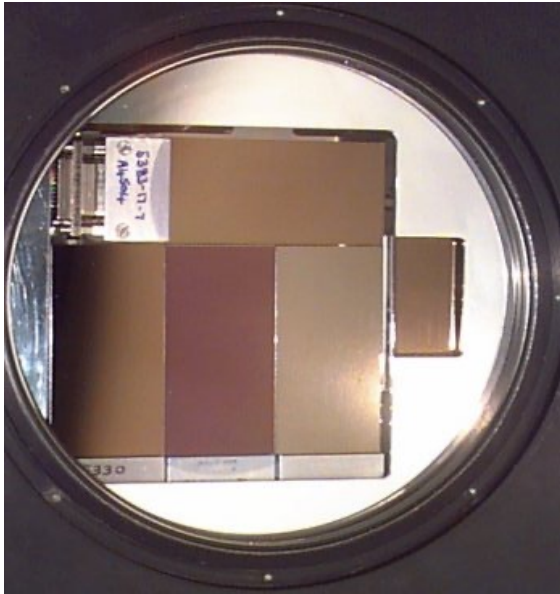


The mosaic mounted in its camera.

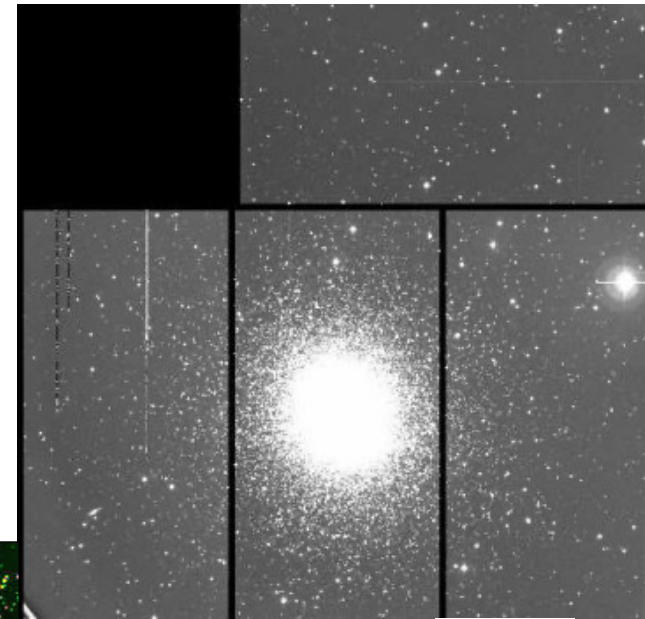


Strumentazione Astronomica: CCD

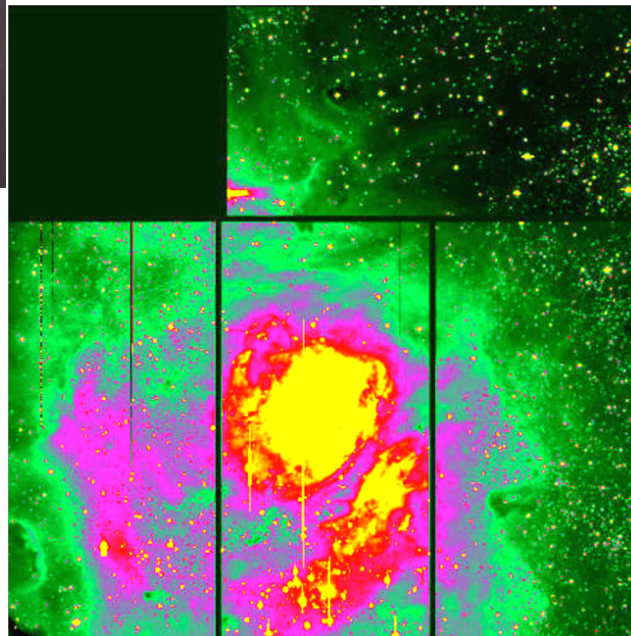
Mosaici di CCD



The INT [Wide Field camera](#) is a [4 Chip Mosaic](#) of thinned AR coated EEV 4K x 2K devices



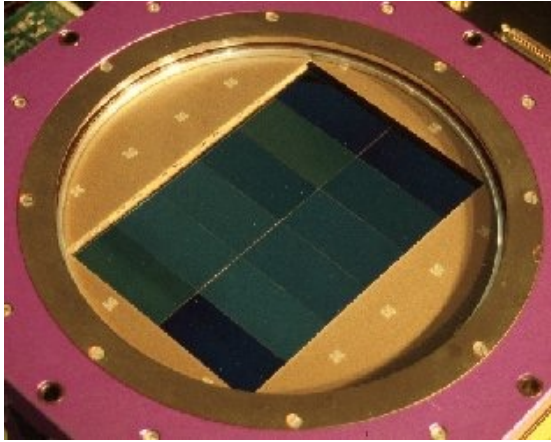
M13



M8

Gli strumenti di piano focale: camere per immagini

Mosaici di CCD



12Kx8K



Picture : Canada France Hawaii Telescope

Strumentazione Astronomica: CCD

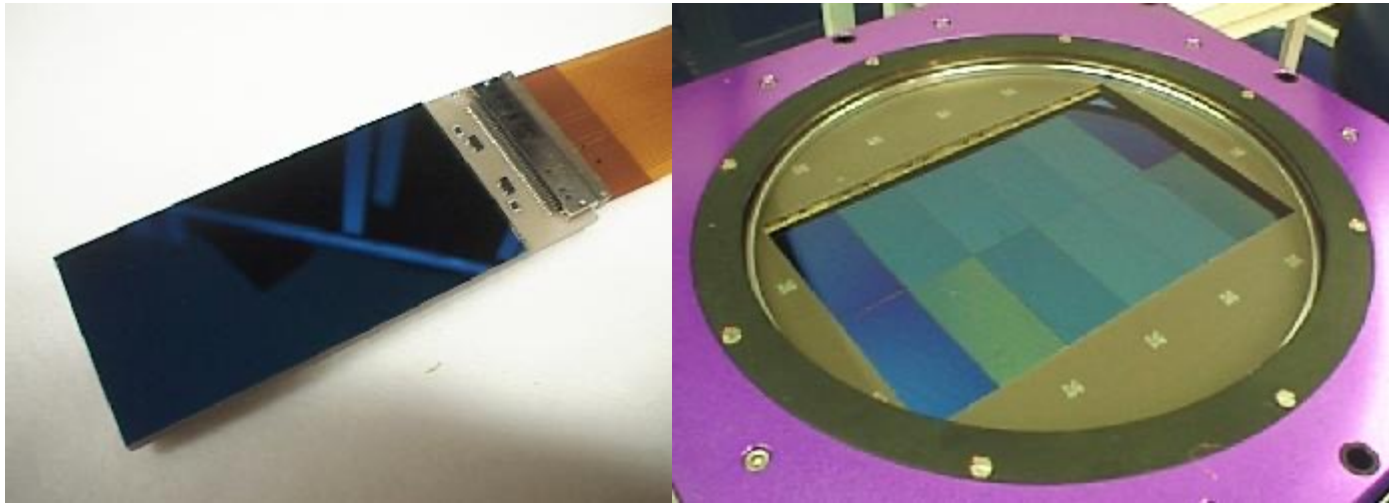
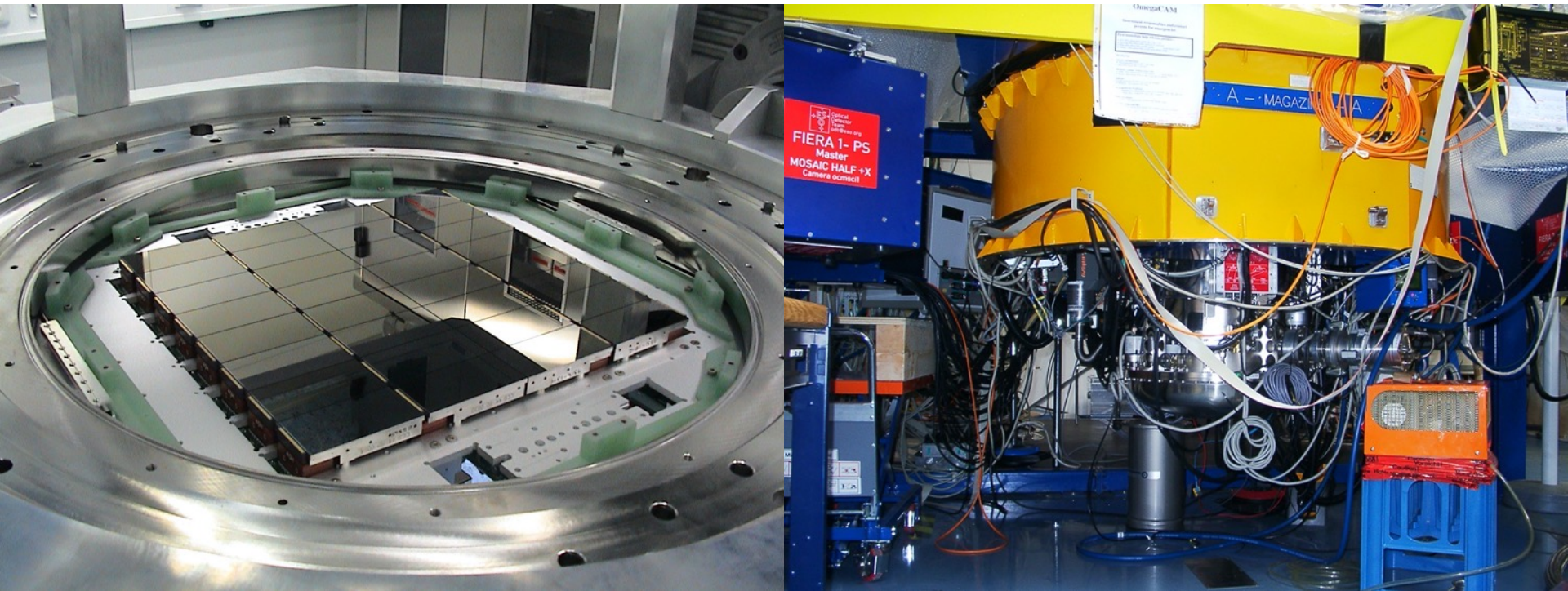


Figure 1 (left): The CCID20 CCD from MIT Lincoln Laboratories, a 2048 by 4096 15 micron pixel thinned device (3.5 cm x 7 cm). Twelve of this model form the CFH12K mosaic.

Figure 2 (right): The CFH12K focal plane: 12,288 by 8,192 pixels, over 100,000,000 pixels! The whole surface (21 by 14 square centimeters) is flat within 40 microns.

Strumentazione Astronomica: CCD

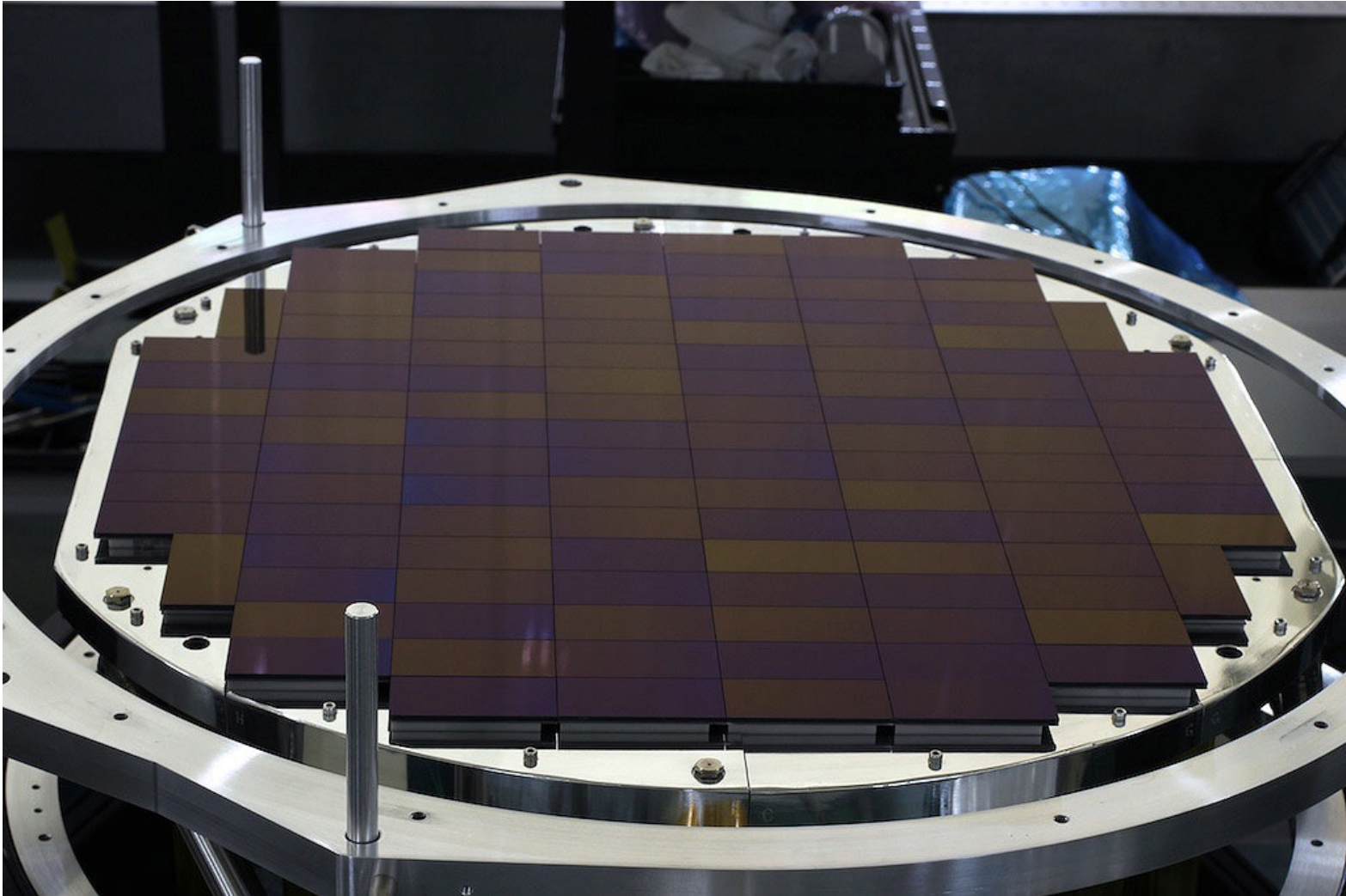
Mosaici di CCD (16kx16k – 256Mpx)



Omega-Cam 16kx16k @ VST Paranal

Strumentazione Astronomica: CCD

Hyper-SuprimeCam 100 CCD per Subaru Telescope



Strumentazione Astronomica: CCD

Table 3.1. *Some CCDs available at the European Southern Observatory (ESO)*

Instrument	Telescope	Type	CCD	Size (pixels)	Pixel Size (microns)	Pixel Scale (arcsec)	Readout Time (seconds)	Gain (e ⁻ /ADU)	Read Noise electrons	Notes
EMMI	3.6-m NTT	Spectrograph Red channel	MIT/LL	2048 × 4096	15	0.17	18–48	1.4	4	Thinned, back-side
EMMI	3.6-m NTT	Spectrograph Blue channel	MIT/LL	1024 × 1024	24	0.37	40	1.4, 2.8	7	Thinned, back-side
FORS2	8-m VLT	Imager/ Spectrograph	MIT/LL	2048 × 4096	15	0.12	40	1.1	6	Deep Depletion, Red optimized
OmegaCam	2.6-m VST	Wide-Field imager	E2V	2048 × 4096	15	0.21	45	3	5	

Table 3.2. *Typical Properties of Two Old and Six Modern Example CCDs*

	RCA	TI	Kodak	E2V	SITe	Sarnoff	STA (WIYN)	MIT/LL
Pixel Format	320 × 512	800 × 800	2048 × 2048	2048 × 4608	2048 × 2048	600 × 2400	3840 × 3952 OT	2048 × 4096
Pixel Size (microns)	30	15	9	13	12	13	12	15
Detector Size (mm)	10 × 15	12 × 12	18 × 18	27 × 62	25 × 25	6 × 25	50	31 × 62
Pixel Full Well (e ⁻)	350 000	50 000	100 000	150 000	110 000	> 20 000	> 70 000	> 200 000
Illumination	Front	Back	Front	Back	Back	Back	Back	Back
Peak QE (%) / Wavelength (Å)	70/4500	70/6500	45/6500	90/5000	85/6500	99/6600	96/5500	95/7700
Read Noise (e ⁻)	80	15	15	3	6	6	< 5	2.5
CTE	0.99995	0.999985	0.99998	0.999995	0.99999	0.99999	0.999998	0.999995
Operating Temp (C)	-100	-120	-30	-85	-85	-60	-60	-110
Typical Gain used (e ⁻ /ADU)	13.5	5	5	1.5	3	5	1.5	1.37

Strumentazione Astronomica: CCD

Table 4.2. *Some Present and Planned Large Telescope CCD Imagers (* marks planned imagers)*

Name	Telescope	Field of View	Focal Plane CCDs	Pixel Size (microns)	Pixel Scale ("'/pix)	Website
MageCam	CFHT	0.92 sq. degrees	40 – 2048 × 4612 E2V	13.5	0.185	http://www.cfht.hawaii.edu/Instruments/Imaging/Megacam/
QUEST	Palomar 48" Schmidt	16 sq. degrees	112 – 600 × 2400 Sarnoff	13	~ 1.5	http://www.astro.caltech.edu/~george/pq/
SUPRIME	Subaru	0.24 sq. degrees	10 – 2048 × 4096 MIT/LL	15	0.2	http://www.naoj.org/Observing/Instruments/SCam/
Mosaic	KPNO/CTIO 4-m	0.36 sq. degrees	8 – 2048 × 4096 SITe	15	0.26	http://www.noao.edu/kpno/mosaic
MegaCam	MMT	0.16 sq. degrees	32 – 2048 × 4096 E2V	15	0.087	http://cfa-www.harvard.edu/~bmcLeod/Megacam/
Dark Energy Camera*	CTIO 4-m	2.9 sq. degrees	70 – 2048 × 4096 LBL	15	0.28	http://www.fnal.gov/pub/
OmegaCam [†]	VST	1.0 sq. degrees	32 – 2048 × 4096 E2V	15	0.21	http://www.eso.org/instruments/omegacam/
One Degree Imager*	WIYN	1.0 sq. degrees	(OTA) 60 – 3840 × 3952 STA/Dalsa	12	0.11	http://www.noao.edu/wiyn/ODI/
Pan-STARRS*	1.8-m	7.0 sq. degrees	(OTA) 60 – 4096 × 4096 MIT/LL	12	0.3	http://pan-starrs.ifa.hawaii.edu/public/index.html
Kepler* (Spacecraft)	1.0-m Schmidt	105 sq. degrees	42 – 2200 × 1024 E2V	27	4	http://www.kepler.arc.nasa.gov/
LSST Camera*	LSST	9.6 sq. degrees	3 Gigapixels LBL	10	0.2	http://www.lsst.org/lsst_home.shtml

Strumentazione Astronomica: CCD

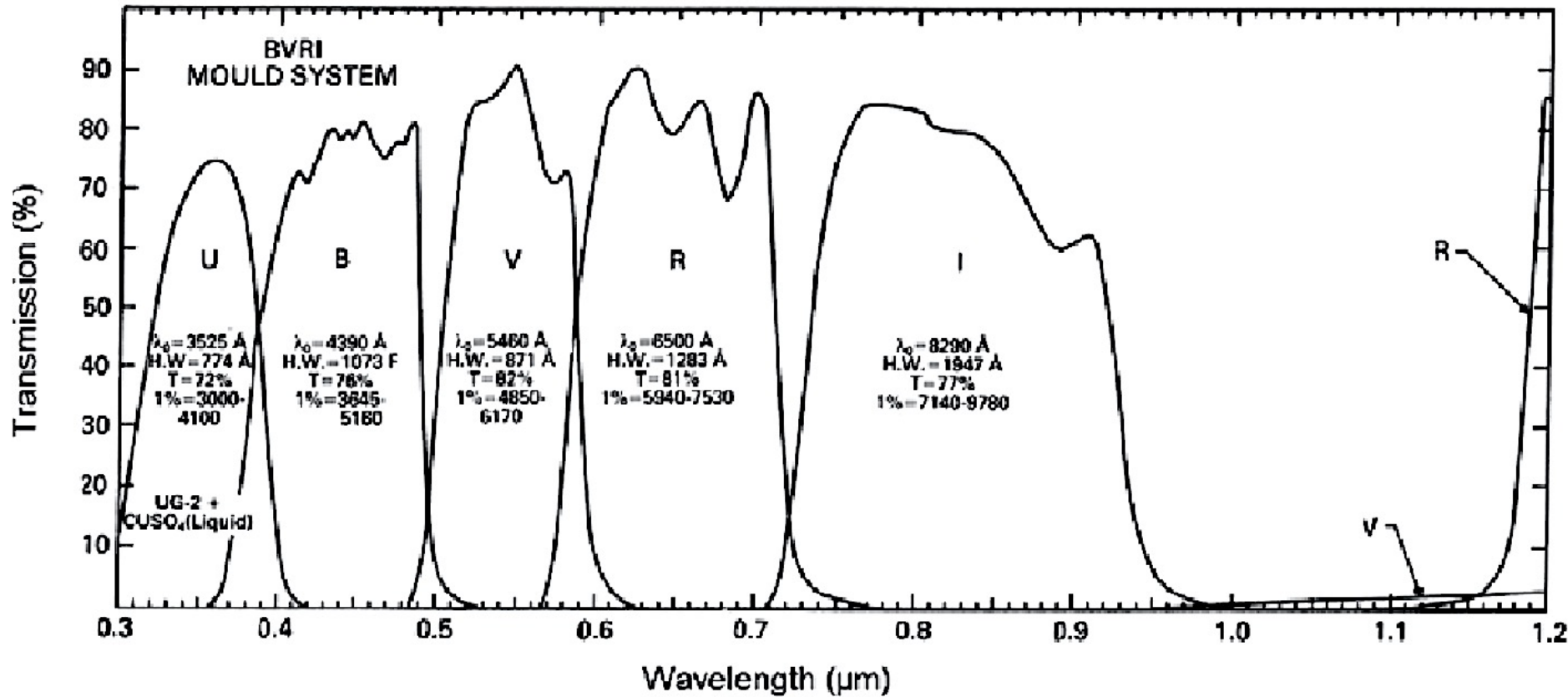


Figure 9.10. Standard filter bandpasses used with CCDs: the Mould system.

Strumentazione Astronomica: CCD

Table 9.4. Absolute flux from a zero-magnitude star like Vega.

<i>Symbol</i>	λ (μm)	ν (Hz)	F_λ ($\text{W cm}^{-2} \mu\text{m}^{-1}$)	F_ν (Jy)*
U	0.36	8.3×10^{14}	4.35×10^{-12}	1,880
B	0.43	7.0×10^{14}	7.20×10^{-12}	4,440
V	0.54	5.6×10^{14}	3.92×10^{-12}	3,810
R	0.70	4.3×10^{14}	1.76×10^{-12}	2,880
I	0.80	3.7×10^{14}	1.20×10^{-12}	2,500
J	1.25	2.4×10^{14}	2.90×10^{-13}	1,520
H	1.65	1.8×10^{14}	1.08×10^{-13}	980
K	2.2	1.36×10^{14}	3.8×10^{-14}	620
L	3.5	8.6×10^{13}	6.9×10^{-15}	280
M	4.8	6.3×10^{13}	2.0×10^{-15}	153
N	9.1	3.0×10^{13}	1.09×10^{-16}	37

* These units are called jansky. One jansky equals $10^{-26} \text{ W m}^{-2} \text{ Hz}^{-1}$, or $(3 \times 10^{-16}/\lambda^2) \text{ W cm}^{-2} \mu\text{m}^{-1}$ if λ is expressed in microns.

Strumentazione Astronomica: CCD

$$\text{CCD EQUATION: } \frac{S}{N} = \frac{N_*}{\sqrt{N_* + n_{pix}(N_B + N_D + N_R^2)}}$$

N_* = # totale di fotoni (elettroni) raccolti

n_{pix} = # di pixel coinvolti

N_B = # totale di fotoni (elettroni) di background per pixel

N_D = # totale di "fotoni" di buio per pixel

N_R = # totale di elettroni per pixel dovuti a readout noise

$$\frac{S}{N} = \frac{N_*}{\sqrt{N_* + n_{pix} \left(1 + \frac{n_{pix}}{n_b} \right) (N_B + N_D + N_R^2 + G^2 \sigma_f^2)}}$$

Experimental Astronomy [0922-6435]
Merline, W J anno:1995 vol:6 fasc:1-2 pag:163
-210

n_b = # di pixel di background coinvolti

G = CCD Gain

σ_f = stima dell'errore introdotto dall'AD converter ~ 0.289

Strumentazione Astronomica: CCD

$$SNR = \frac{S \cdot n_o \cdot t}{\sqrt{S \cdot n_o \cdot t + n_{pix} (B \cdot n_o \cdot t + D \cdot n_o \cdot t + n_o R^2)}} \quad n_o \text{ OBJECT FRAMES}$$

1. *Background-limited or “sky-limited” case:* $\frac{S}{N} = S\sqrt{T} [(n_{pix} B)]^{-1/2}$

$$S/\sqrt{B} \sim D^2/D = D$$

2. *Detector noise-limited case:* $\frac{S}{N} = \frac{S\sqrt{T}}{\left[n_{pix} \left(\frac{R^2}{t} \right) \right]^{1/2}} = \frac{St}{R} \sqrt{\frac{n_o}{n_{pix}}} \sim D^2$

Strumentazione Astronomica: CCD

$$\text{FINAL FRAME} = \frac{\text{OBJECT FRAME} - \text{DARK FRAME}}{\text{FLAT FRAME} - \text{DARK FRAME}}$$

BIAS FRAME

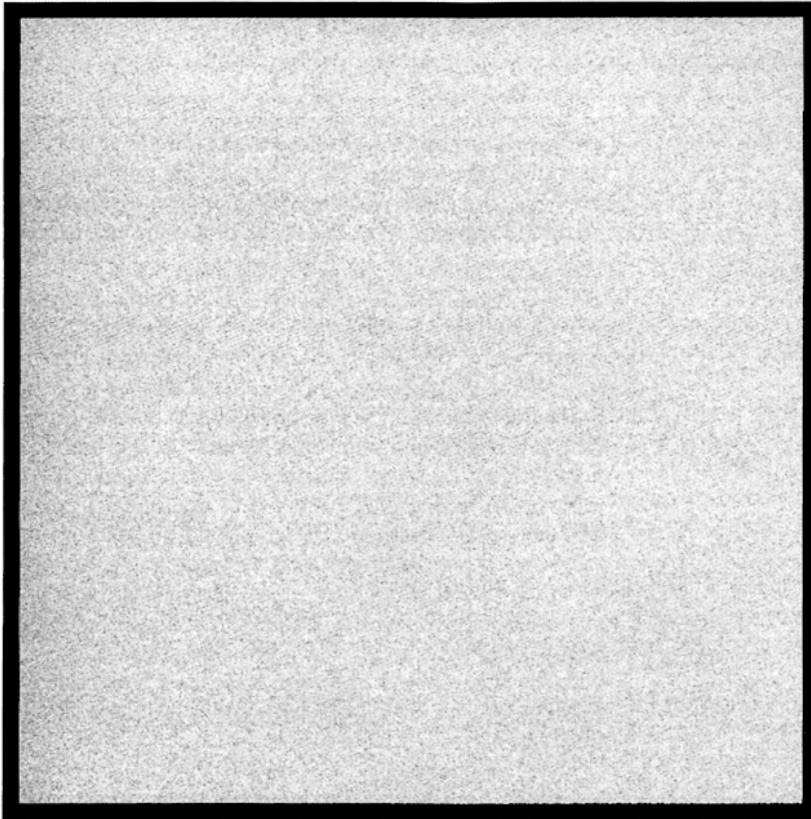


Fig. 4.2. Shown is a typical CCD bias frame. The histogram of this image was shown in Figure 3.8. Note the overall uniform structure of the bias frame.

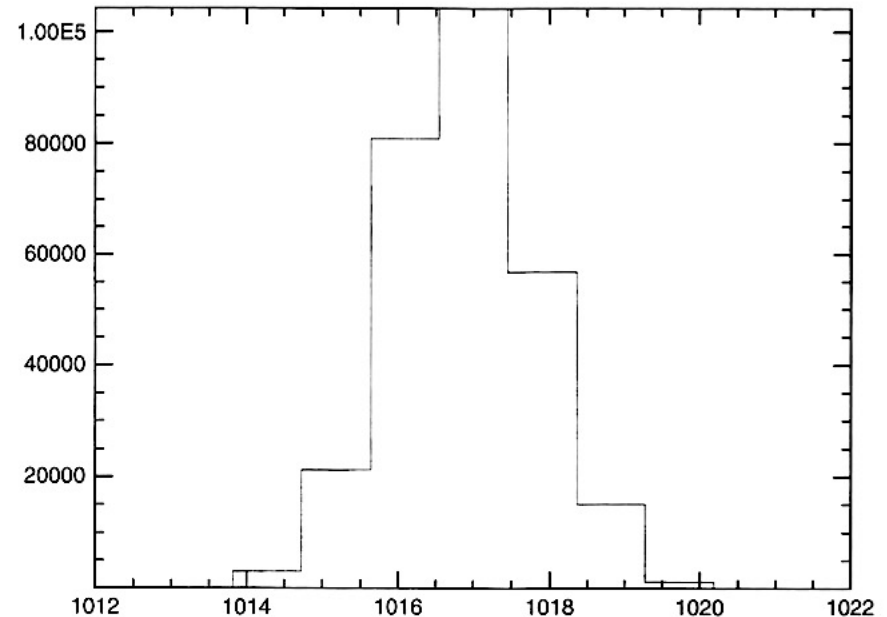
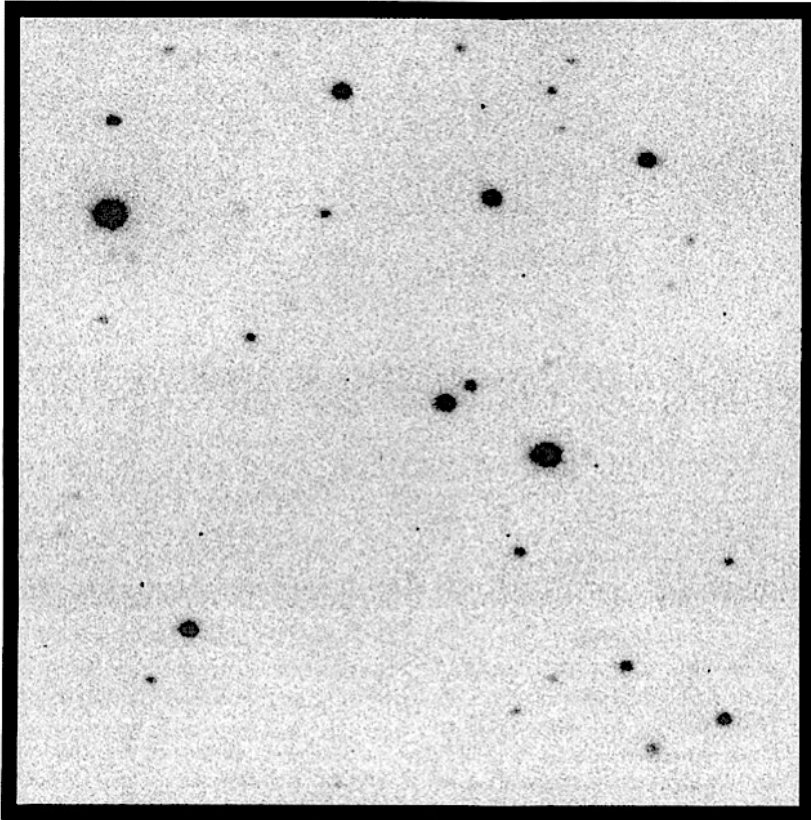


Fig. 3.8. Histogram of a typical bias frame showing the number of pixels vs. each pixel ADU value. The mean bias level offset or pedestal level in this Loral CCD is near 1017 ADU, and the distribution is very Gaussian in nature with a FWHM value of near 2 ADU. This CCD has a read noise of 10 electrons and a gain of $4.7e^-/\text{ADU}$.

Steve Howell: Handbook of CCD Astronomy
Cambridge University Press (ebook disponibile)

Strumentazione Astronomica: CCD



OBJECT FRAME

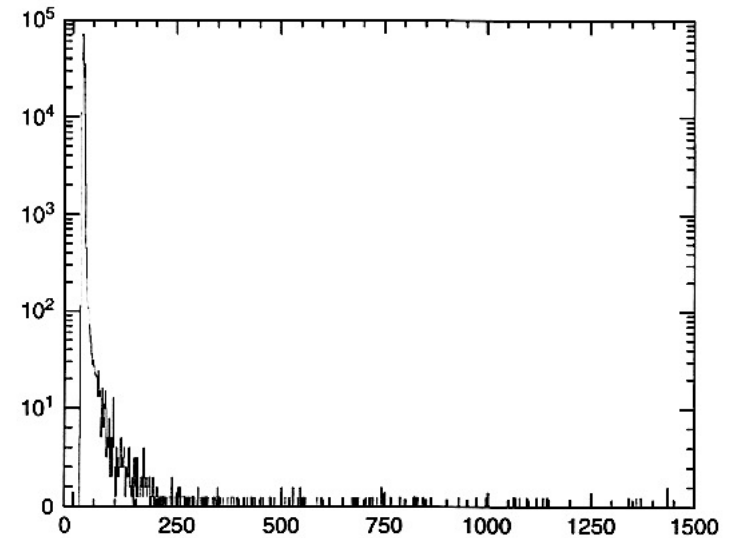
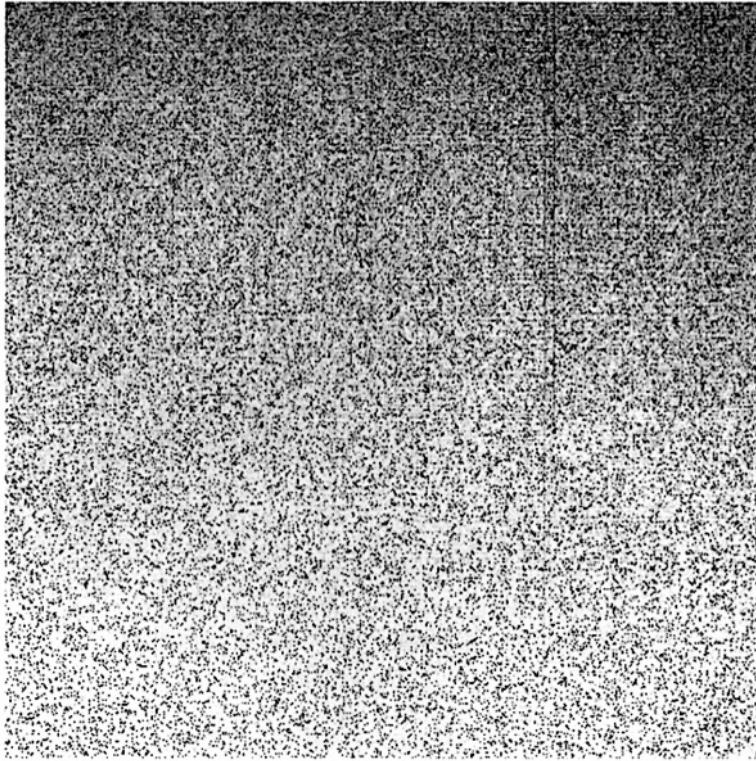


Fig. 4.5. (cont.)

Fig. 4.5. Shown is a typical CCD object frame showing a star field. This image has been properly reduced using bias frame subtraction and division by a flat field image. Note how the background is of a uniform level and distribution; all pixel-to-pixel nonuniformities have been removed in the reduction process. The stars are shown as black in this image and represent R magnitudes of 15th (brightest) to 20th (faintest). The histogram shown in the remainder of the figure is typical for a CCD object frame after reduction. The large grouping of output values on the left (values less than about 125 ADU) are an approximate Gaussian distribution of the background sky. The remaining histogram values (up to 1500 ADU) are the pixels that contain signal levels above the background (i.e., the pixels within the stars themselves!).

Strumentazione Astronomica: CCD



DARK FRAME

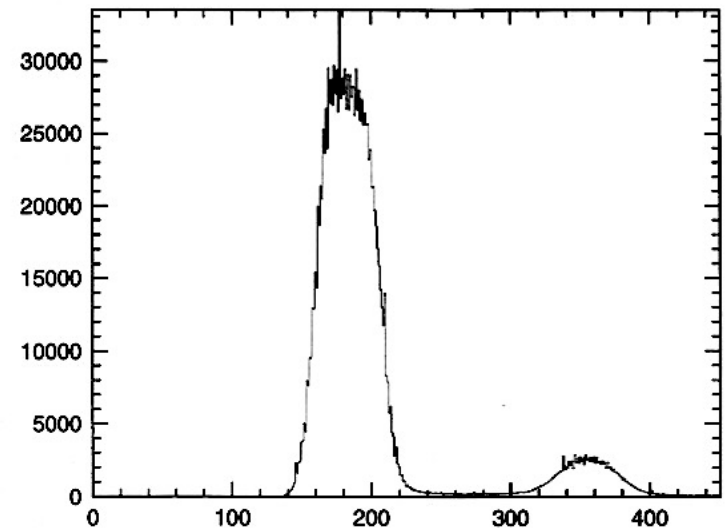


Fig. 4.3. (cont.)

Fig. 4.3. Shown is a typical CCD dark frame. This figure shows a dark frame for a Kodak CCD operating in MPP mode and thermoelectrically cooled. Notice the nonuniform dark level across the CCD, being darker (greater ADU values) on the top. Also notice the two prominent partial columns with higher dark counts, which extend from the top toward the middle of the CCD frame. These are likely to be column defects in the CCD that occurred during manufacture, but with proper dark subtraction they are of little consequence. The continuation of the figure shows the histogram of the dark frame. Most of the dark current in this 180 second exposure is uniformly distributed near a mean value of 180 ADU with a secondary maximum near 350 ADU. The secondary maximum represents a small number of CCD pixels that have nearly twice the dark current of the rest, again most likely due to defects in the silicon lattice. As long as these increased dark current pixels remain constant, they are easily removed during image calibration.

Strumentazione Astronomica: CCD

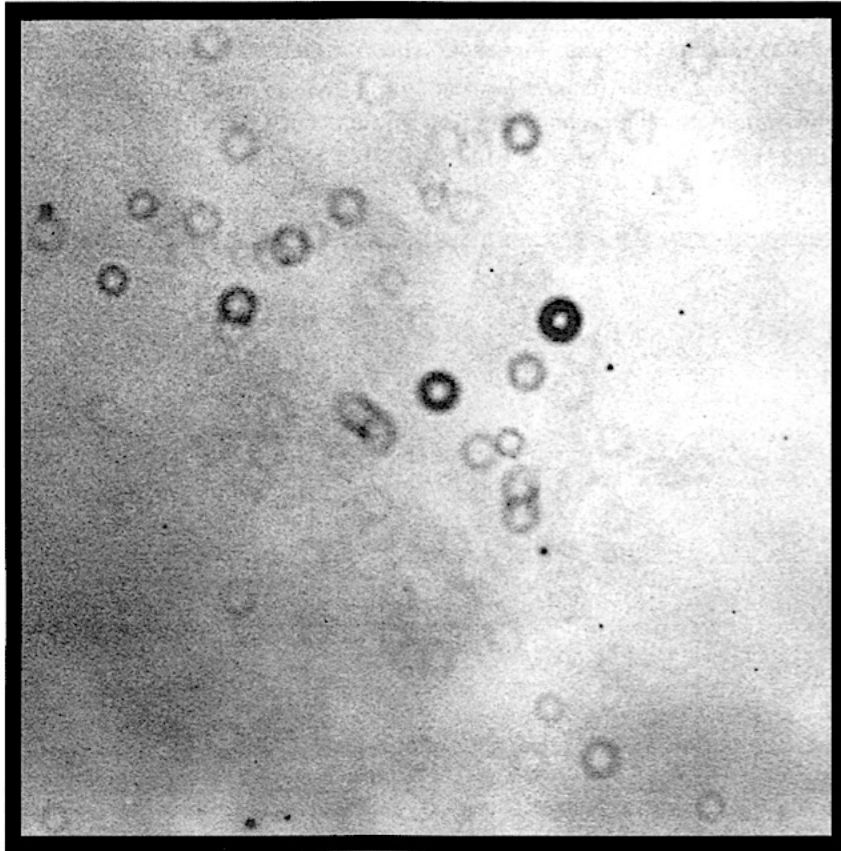


Fig. 4.4. Shown is a typical CCD flat field image. This is an R-band flat field image for a 1024×1024 Loral CCD. The numerous "doughnuts" are out of focus dust specks present on the dewar window and the filter. The varying brightness level and structures are common in flat field images. As seen in the histogram of this image (Figure 4.1) this flat field has a mean level near 6950 ADU, with an approximate dispersion of (FWHM) 400 ADU.

FLAT FIELD FRAME

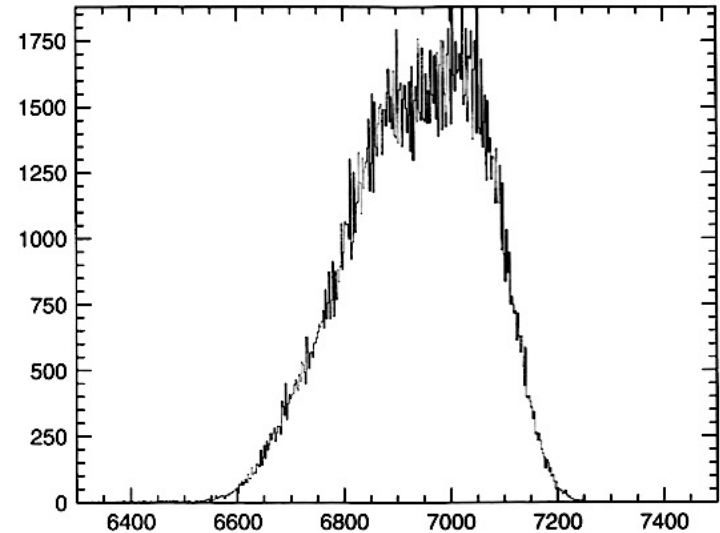


Fig. 4.1. Histogram of a typical flat field image. Note the fairly Gaussian shape of the histogram and the slight tail extending to lower values. For this R-band image, the filter and dewar window were extremely dusty leading to numerous out of focus "doughnuts" (see Figure 4.4), each producing lower than average data values.

Strumentazione Astronomica: MCP

MULTI-ANODE MICROCHANNEL ARRAY
four-fold coincidence-anode array

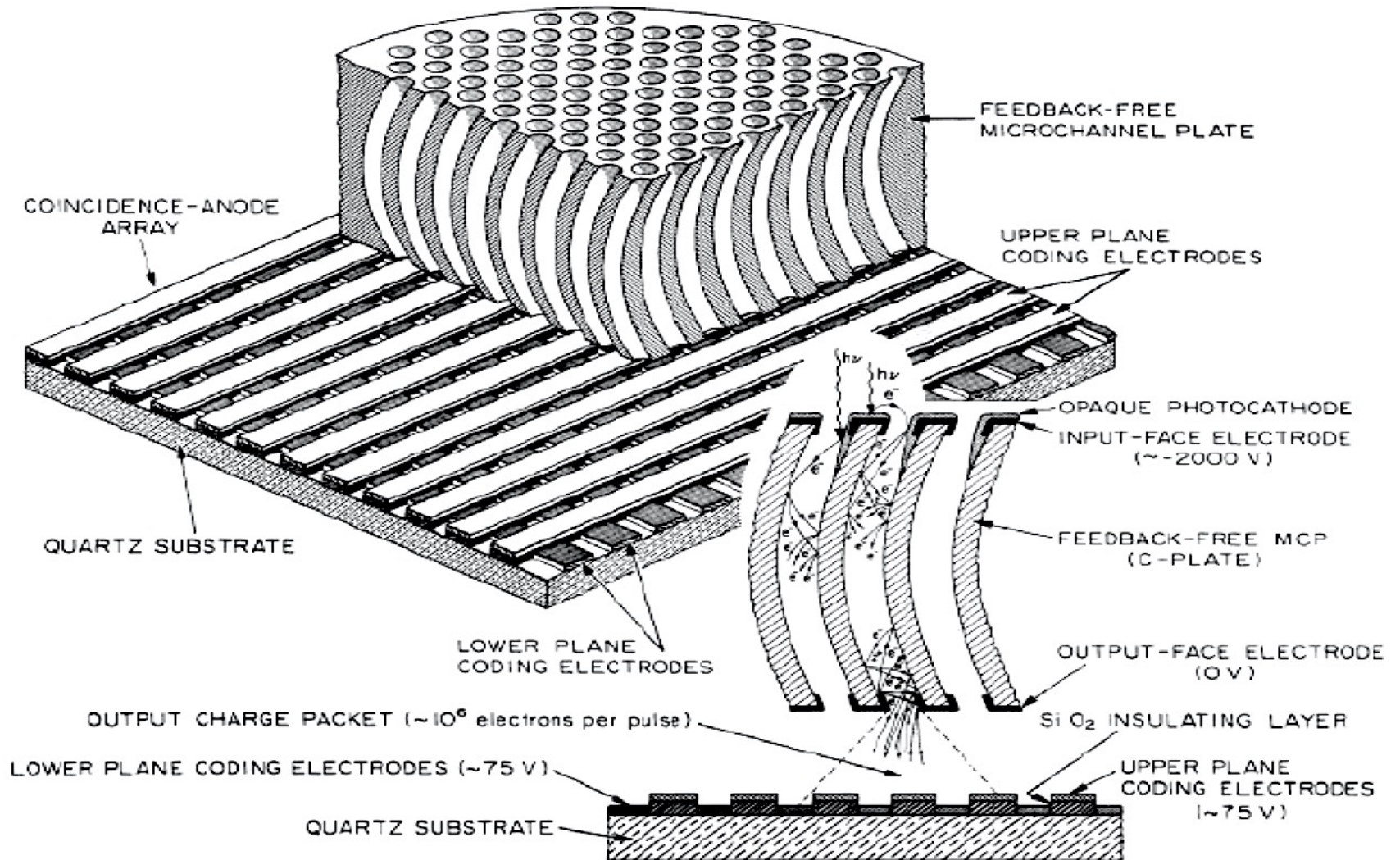
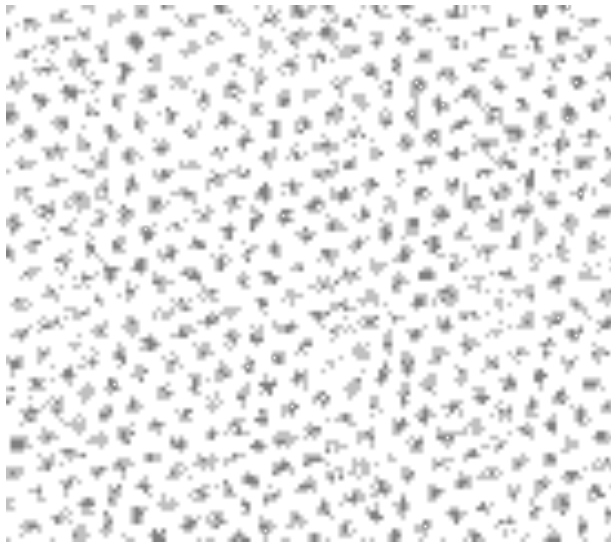
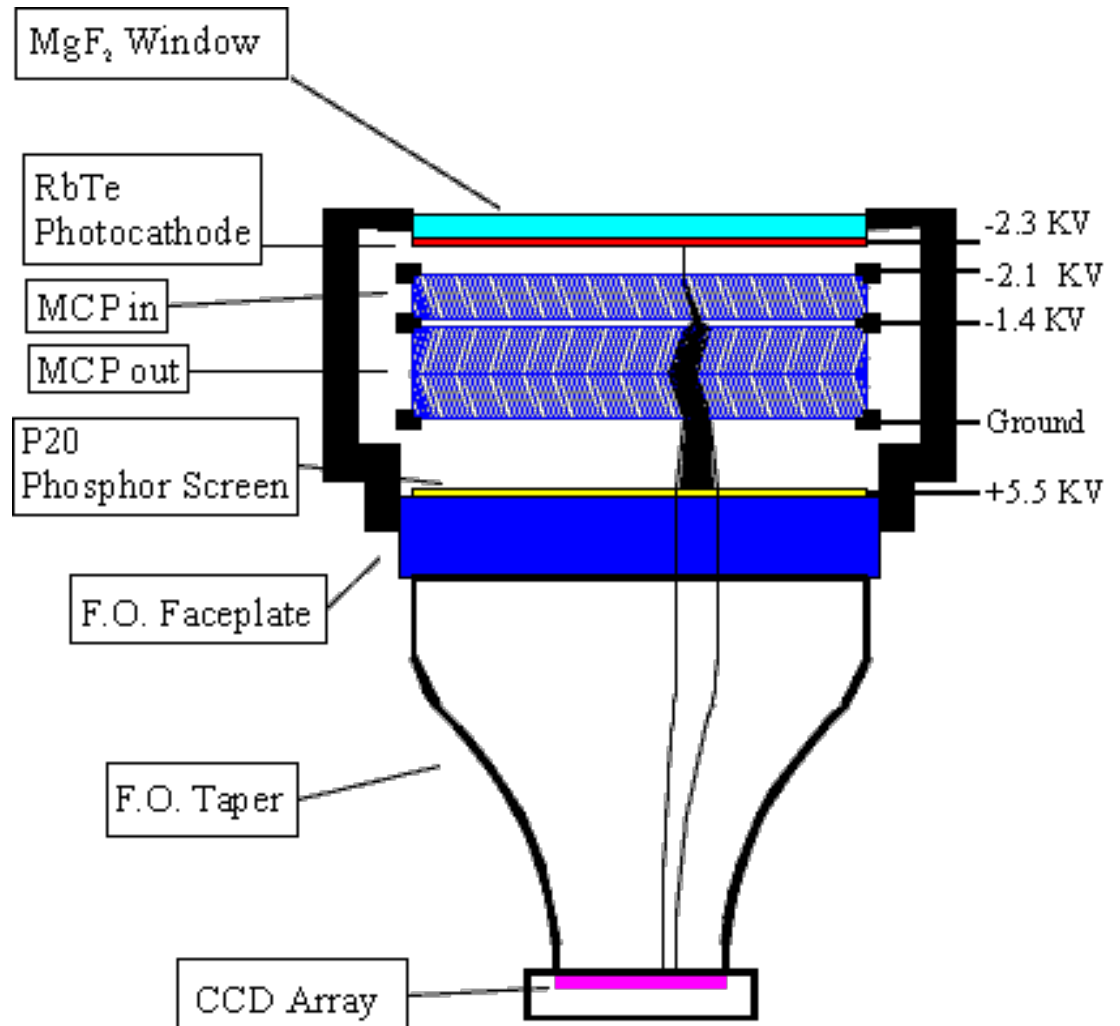


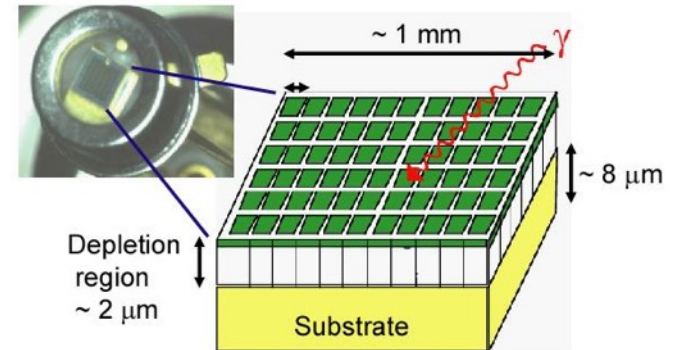
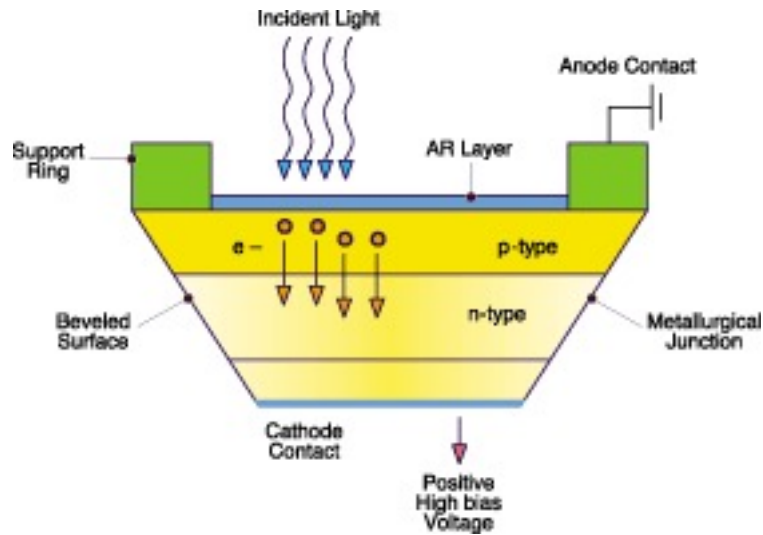
FIG. 16—Schematic of a multilayer coincidence-anode array.
Strumentazione Astronomica - Camere per
Immagini 2021

Strumentazione Astronomica: MCP

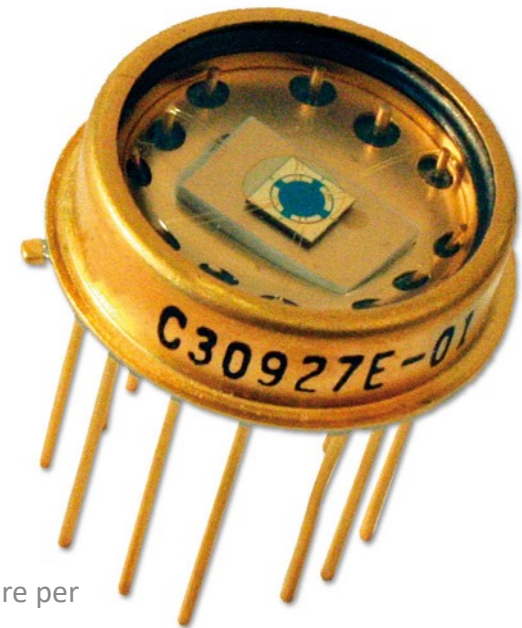
• *Micro-Channel Plate*
letto tramite un fosforo
e un CCD



Strumentazione Astronomica: APD



Velocissimi RT~ns



Telescopi infrarossi

Da terra:

- UKIRT (3.8m) 0.8 – 5 μm (Mauna Kea 4205m)
- VISTA (4.1m) 0.85 – 2.3 μm (Paranal 2635m)
- NASA IRTF (3m) 0.8 – 25 μm (Mauna Kea 4205m)
- TAO (6.5m) 1 – 38 μm (Atacama Cerro Chajnantor 5640m)
- SUBARU (8.2m) 0.8 – 25 μm (Mauna Kea 4205m)

In quota stratosferica: SOFIA (2.5m) 0.8-160 μm ~20km

Dallo Spazio:

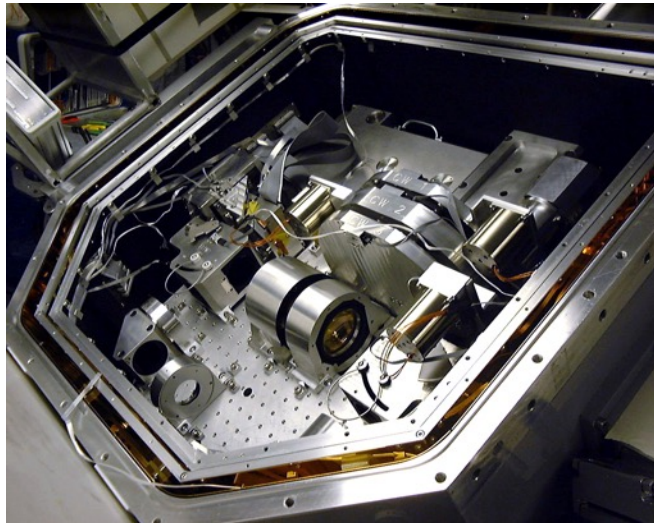
- ISO (0.6m) 2.5-240 μm
- HERSCHEL (3.5m) 60-672 μm
- SPITZER (0.85m) 3-180 μm
- JWST (6.5m) 0.6-28.5 μm
- HST (2.5m) 0.8 – 2.5 μm

Tre esempi

SUBARU

Suprime-Cam

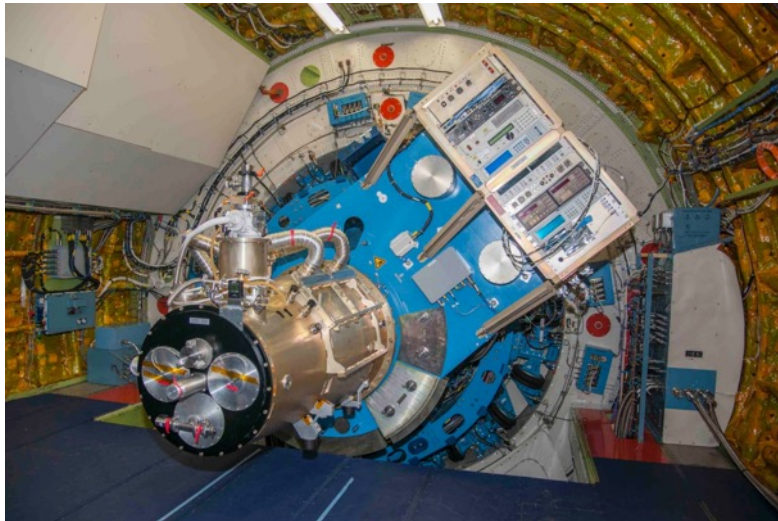
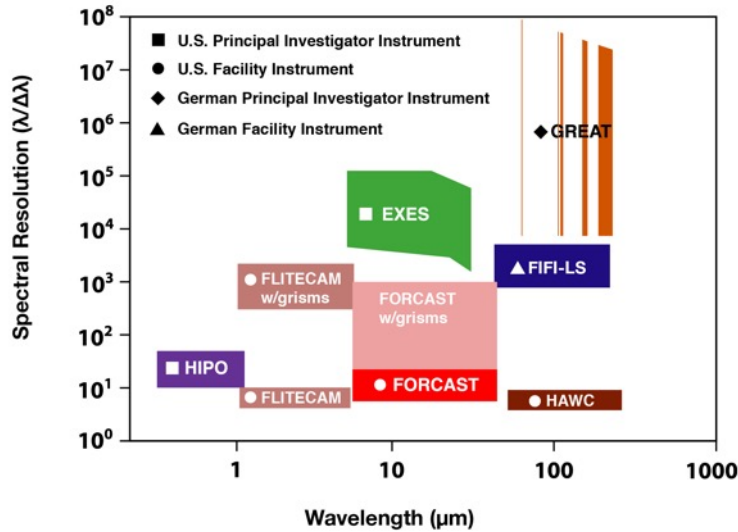
Camera al fuoco primario



IRCS Infrared Camera
and Spectrograph



SOFIA: Stratospheric Observatory for Infrared Astronomy



Array 8x8 di rivelatori eterodina
Stratospheric Heterodyne Array System for
Terahertz Astronomy, (SHASTA)

JWST

Underside of the James Webb Space Telescope

Cold side of telescope:
~40°K
(~ -388°F)

Segmented primary mirror
Eighteen hexagonal segments made of the metal beryllium and coated with gold to capture infrared light

Multi-layer sunshield
Five layers shield the observatory from the light and heat from the Sun and Earth

Trim flap
Helps stabilize the satellite

Star trackers
Small telescopes that use star patterns to target the observatory

Solar power array
Always facing the Sun, panels convert sunlight into electricity to power the observatory

Spacecraft bus
Contains most of the spacecraft steering and control machinery, including the computer and the reaction wheels

Earth-pointing antenna
Sends science data back to Earth and receives commands from NASA's Deep Space Network

The ISIM system consists of:

- Four science instruments
- Nine instrument support systems:
 - Optical metering structure system
 - Electrical Harness System
 - Harness Radiator System
 - ISIM electronics compartment (IEC)
 - Cryogenic Thermal Control System
 - ISIM Command and Data Handling System (ICDH)
 - ISIM Remote Services Unit (IRSU)
 - Flight Software System
 - Operations Scripts System

